NANOSYSTEMS: PHYSICS, CHEMISTRY, MATHEMATICS, 2020, 11 (2), P. 246–251

Influence of hydrothermal synthesis conditions on the composition of the pyrochlore phase in the Bi_2O_3–Fe_2O_3–WO_3 system

M. S. Lomakin[1,2], O. V. Proskurina[1,2], V. V. Gusarov[1]

[1]Ioffe Institute, 26, Politekhnicheskaya St., 194021, St. Petersburg, Russia

[2]St. Petersburg State Institute of Technology, 26, Moskovsky pr, 190013, St. Petersburg, Russia

lomakinmakariy@gmail.com

DOI 10.17586/2220-8054-2020-11-2-246-251

The paper deals with a study of the effect which the hydrothermal fluid pH has on the formation of a pyrochlore-structured phase in the Bi_2O_3–Fe_2O_3–WO_3 system. It was shown that at pH of 1 and 8, the formation of pyrochlore-structured phase particles with crystallite sizes of 38 and 118 nm, respectively, is accompanied by the formation of the Bi_2WO_6 compound with the Aurivillius phase structure. At pH values from 2 to 7, only pyrochlore-structured nanocrystalline particles with a variable composition are formed. Under these conditions, the dependence of the average size of crystallites of the pyrochlore-structured phase particles on pH is extreme, as the size increases from $\sim$ 67 nm at pH 2 up to $\sim$ 126 nm at pH 5 and then decreases to $\sim$ 102 nm at pH 7. The samples obtained at pH 3–4 have a composition that is the closest to that specified for the synthesis. When pH increases up to 10, there forms a non-single-phase product that contains the Bi_2WO_6 phase and δ-Bi_2O_3-based phase.

Keywords: hydrothermal synthesis, pyrochlore phase, nanocrystals, crystallite size.

Received: 14 January 2020

Revised: 28 February 2020

1. Introduction

As a rule, the conditions of hydrothermal synthesis (HTS), significantly affect the composition, structure, and size of particles and crystallites of the synthesized products [1–7]. Important factors in this case are the sequence and rate of reagents mixing and the pH of the hydrothermal fluid [8, 9]. Changes in pH usually significantly affect the state and composition of phases resulting from hydrothermal treatment [10, 11]. Another important factor is the effect of pH on the change in the structure of the double electric layer on the surface of solid phase particles, which, in turn, can determine the crystallite growth mechanisms, the possibility and rate of particles aggregation, their shape and size [12, 13]. The pH of the medium has a particularly strong effect on phase equilibria in the systems containing W^{6+} ions, which are characterized not only by changes in the composition and structure of aqueous complexes with a change in pH, but also by the condensation of acid residues into a sparingly soluble isopolyacid in a highly acidic media [14]. Other examples are bismuth (III) and iron (III) hydroxides, the degree of hydration of which depends on the pH of the medium [15,16], and the pH at the onset of hydrates formation varies from $\sim$ 1.5 for iron hydroxide up to $\sim$ 3.2 for bismuth hydroxide [16]. The HTS method application in [17] has for the first time resulted in producing and characterizing a pyrochlore-structured phase with the variable composition $Bi_{y+0.67\delta}Fe_yW_{2-y}O_6O'_\delta$ (BFWO) in two-phase mixtures. The preparation of BFWO-based single-phase samples with a specified composition has encountered a number of synthesizing difficulties that require a systematic study of the influence of phase formation conditions on the composition and structure of the target product.

This work is aimed at establishing optimal pH values of the hydrothermal fluid for the synthesis of BFWO nanocrystalline phases with a specified composition.

2. Materials and methods

2.1. Synthesis section

The molar ratio of the reagents was chosen based on the stoichiometry of the target product, i.e., a pyrochlore-structured phase with the $Bi_{0.5}Fe_{0.36}WO_{4.29}$ composition. The synthesis was carried out in several stages. 2 mmol of crystalline bismuth (III) nitrate pentahydrate, $Bi(NO_3)_3{\cdot}5H_2O$ (puriss. spec.), were dissolved in 30 ml of 1M HNO_3 (puriss. spec.) by stirring with a magnetic stirrer until complete dissolution, and 1.44 mmol of crystalline iron(III) nitrate nonahydrate, $Fe(NO_3)_3{\cdot}9H_2O$ (pur.), were added to the resulting bismuth nitrate solution. The dissolution of the iron salt was very fast. 4 mmol of crystalline hydrate (VI) of sodium tungstate, $Na_2WO_4{\cdot}2H_2O$ (p.a.), were dissolved in 25 ml of distilled water and then added dropwise to the continuously stirred solution of bismuth and iron salt. After an hour of continuous stirring of the resulting suspension, NaOH 4M solution was added dropwise to achieve pH 1 (without adding NaOH), 2, 3, ..., 8, 10. After stirring for some more time, the resulting suspension was

transferred to a separate Teflon crucible (80% filling) and placed in a steel autoclave, which was put in a furnace heated up to 200°C. Twenty-four hours later, the autoclave was removed from the furnace and cooled at room temperature. The obtained precipitates were separated in a centrifuge, rinsed with distilled water and dried at 80°C for 24 hours.

2.2. Characterization

The X-ray diffraction (XRD) patterns were recorded at 295 K on a Rigaku SmartLab 3 powder diffractometer ($Co_{K\alpha}$ emission) with the K_β filter in the $2\theta = 15$ to 71° angle range and at a speed of 3°/min. The average size of crystallites was calculated by the Halder–Wagner method. The elemental bulk composition, the morphology and size of the particles were determined using a Tescan Vega 3 SBH scanning electron microscope with an Oxford Instruments X-ray microanalysis attachment. The elemental composition was determined with a 1 mass. % error.

3. Results and discussions

3.1. Obtained samples composition

Bulk compositions of the obtained samples are presented in Table 1. An increase in the hydrothermal fluid pH significantly affects changes in the obtained samples bulk composition.

TABLE 1. Obtained samples bulk composition

Synthesized composition		Bi, at. %	Fe, at. %	W, at. %
		26.9	19.4	53.7
pH	1	28.5	17.2	54.3
	2	27.2	18.5	54.3
	3	26.7	19.4	53.9
	4	26.5	19.7	53.8
	5	27.6	20.1	52.3
	6	30.6	20.0	49.4
	7	32.9	22.6	44.5
	8	37.1	22.9	40.0
	10	45.2	35.9	18.9

The exceptions are the single-phase samples obtained at pH 2, 3, and 4, in which the bismuth/tungsten molar ratio is constant (Bi/W ~ 0.5), and only the amount of iron changes, slightly increasing with the increasing pH. The single-phase samples obtained at pH 5, 6, and 7, demonstrate an increase in the amount of bismuth and iron along with the increasing pH, while the amount of tungsten in the BFWO structure decreases. These facts provide evidence for the presence of a certain region of compositions in the ternary diagram of Bi_2O_3–Fe_2O_3–WO_3, in which the BFWO phase exists, which is thus a phase of variable composition, since a significant change in the elements ratio in the BFWO phase does not lead to the appearance of other phases. It should be noted that the compositions of the samples obtained at pH 3 and 4 correspond to the composition specified for the synthesis to the greatest extent. The bulk compositions of the samples obtained at pH 1, 8, and 10 are found in the non-single-phase region.

3.2. XRD analysis

The crystal structure and phase composition of the obtained samples were analyzed by X-ray powder diffraction technique. The XRD patterns of non-single-phase and single-phase samples are presented in Fig. 1 and Fig. 2, respectively. The XRD pattern of a sample obtained at pH 1 (Fig. 1) shows the presence of the BFWO phase (CSD 1961005) with the average size of crystallites of ~ 38 nm, and of the Bi_2WO_6 phase (ICSD code 73-1126).

Only the BFWO phase is present in the samples obtained at pH 2, 3 and 4 (Fig. 2). The unit cell parameter a of the BFWO phase for these samples varies only slightly and averages 10.3341(5) Å. No other crystalline phases, except for BFWO, were present also in the XRD patterns of the samples obtained at pH 5, 6, and 7 (Fig. 2). The sample obtained at pH 8 mainly consists of the BFWO phase with an average crystallite size of ~ 118 nm, with a small amount of the Bi_2WO_6 phase (Fig. 1). The local microanalysis data for the BFWO phase in the sample obtained at pH 8 does not practically differ from the bulk composition of the sample, since the mass fraction of the Bi_2WO_6 phase in this sample is negligibly small. In this regard, the BFWO phase composition in this sample can be taken equal to the bulk composition of the sample, although with some reservation. The unit cell parameter a of the BFWO phase in the samples synthesized at pH 5, 6, 7, and 8 of the hydrothermal fluid increases with the increasing pH from

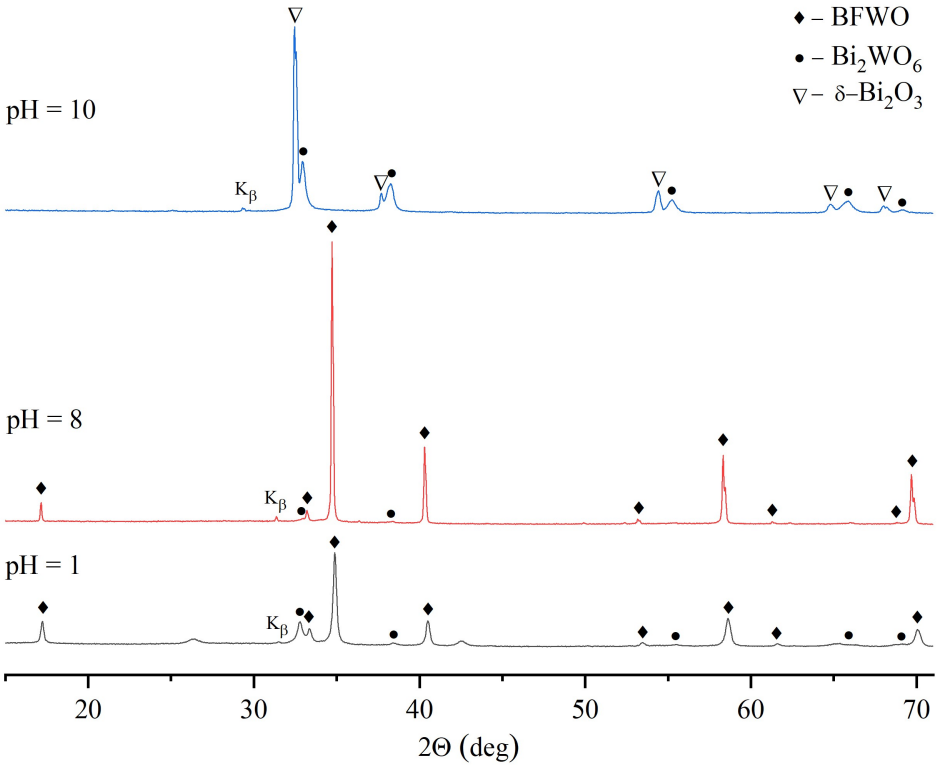

FIG. 1. XRD patterns of the non-single-phase samples obtained at different pH values

10.3394(8) Å (pH 5) up to 10.3848(6) Å (pH 8). The data on the BFWO phase compositions and unit cell parameter are consistent with the data obtained in [17], which state that the unit cell parameter increases with an increase in the amount of bismuth in the pyrochlore structure. According to the X-ray diffraction data on the sample obtained at pH 10 (Fig. 1), two crystalline phases coexist in it, i.e., the Aurivillius-structured Bi_2WO_6 and the δ-Bi_2O_3-based phase (ICSD code 16-654). According to the local microanalysis data, the composition of the δ-Bi_2O_3-based phase is $Bi_{3.35}Fe_{0.68}WO_{9.05}$.

Figure 3 presents the BFWO phase crystallite size as the extreme function of the hydrothermal fluid pH.

3.3. Obtained samples morphology

The SEM data are presented in Fig. 4. The sample obtained at pH 1 consists of particles 100–150 nm in size; individual phases in this sample are morphologically indistinguishable (Fig. 4a). The BFWO phase particles in the samples obtained at pH 2, 3, 4, 6, 7 and 8 have a similar morphology (Fig. 4b). These are spherical agglomerates consisting of crystallites; the size of both depends on the hydrothermal fluid pH. In the sample obtained at pH 5, the agglomerates of the BFWO phase are significantly enlarged and start acquiring the octahedral shape (Fig. 4c). In the sample obtained at pH 8 (Fig. 4d), the Aurivillius phase-structured Bi_2WO_6 compound coexisting with BFWO is represented by spherical agglomerates with a size of ~ 5 μm.

According to the data obtained by SEM in backscattered electrons (Fig. 4f), three phases coexist in the sample obtained at pH 10 (Fig. 4e). The δ-Bi_2O_3-based and the Bi_2WO_6 phases are crystalline, since they differ in the XRD pattern of this sample. The particles of the δ-Bi_2O_3-based phase in the sample obtained at pH 10 are regular octahedrons with a size of ~ 10 μm, but they are not single crystals, since the peaks of this phase have a significant broadening in the XRD pattern (Fig. 1). Particles of the Bi_2WO_6 phase in this sample are represented by fused plates with no pronounced agglomeration, with an average crystallite size of about 23 nm. The third phase in the sample obtained at pH 10, (marked as XR am-us in Fig. 4f), is X-ray amorphous and, according to the local microanalysis, has the composition $Bi_{2.61}Fe_{2.84}WO_{11.18}$, i.e., it is significantly richer in iron, which is also seen from the phase contrast (Fig. 4f).

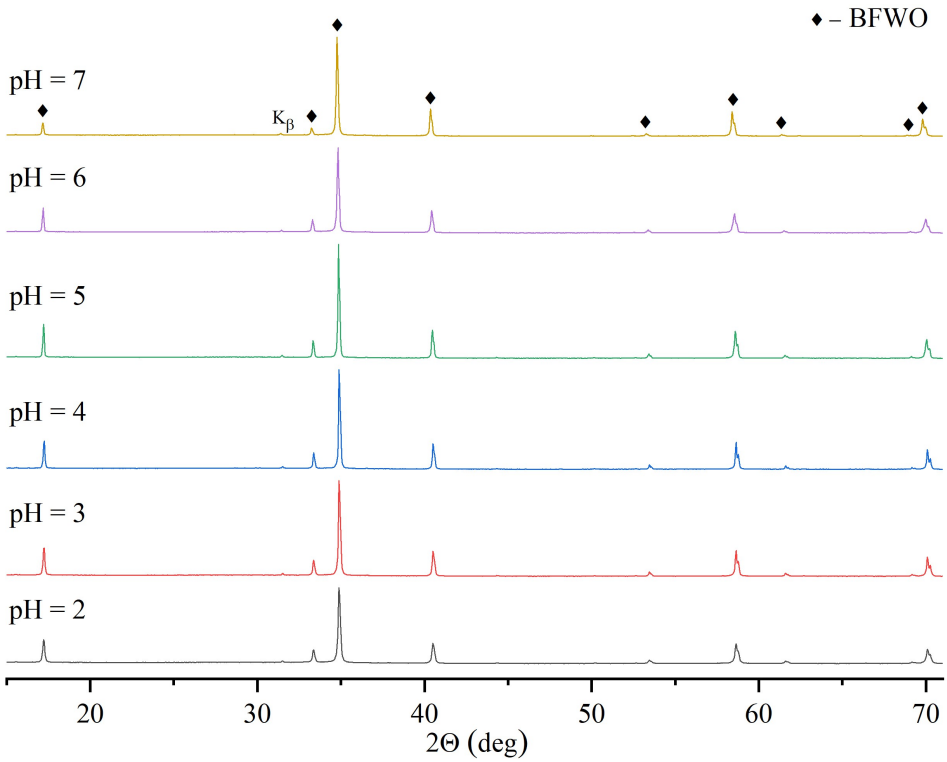

FIG. 2. XRD patterns of the single-phase samples obtained at different pH values

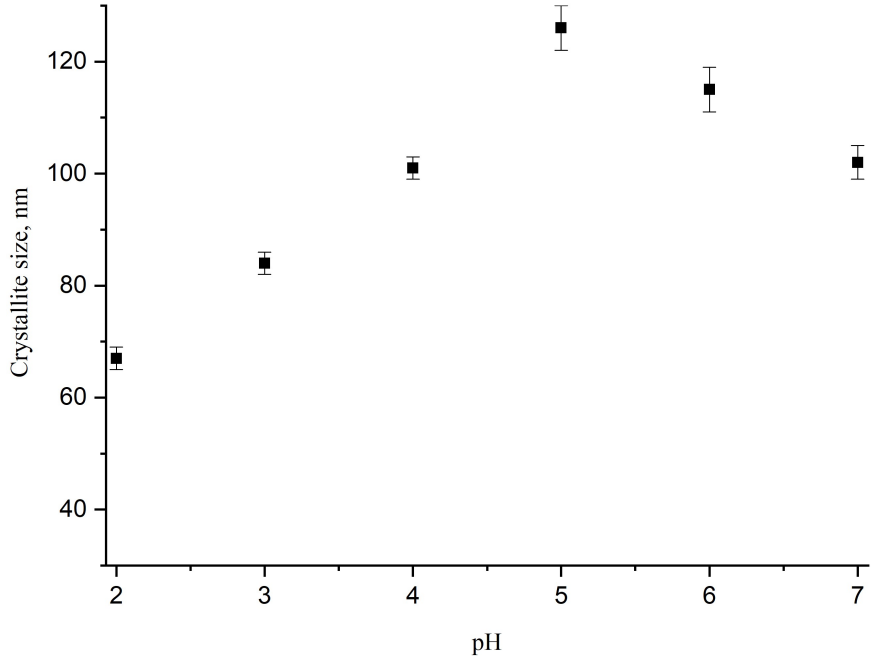

FIG. 3. BFWO phase crystallite size as the function of the hydrothermal fluid pH

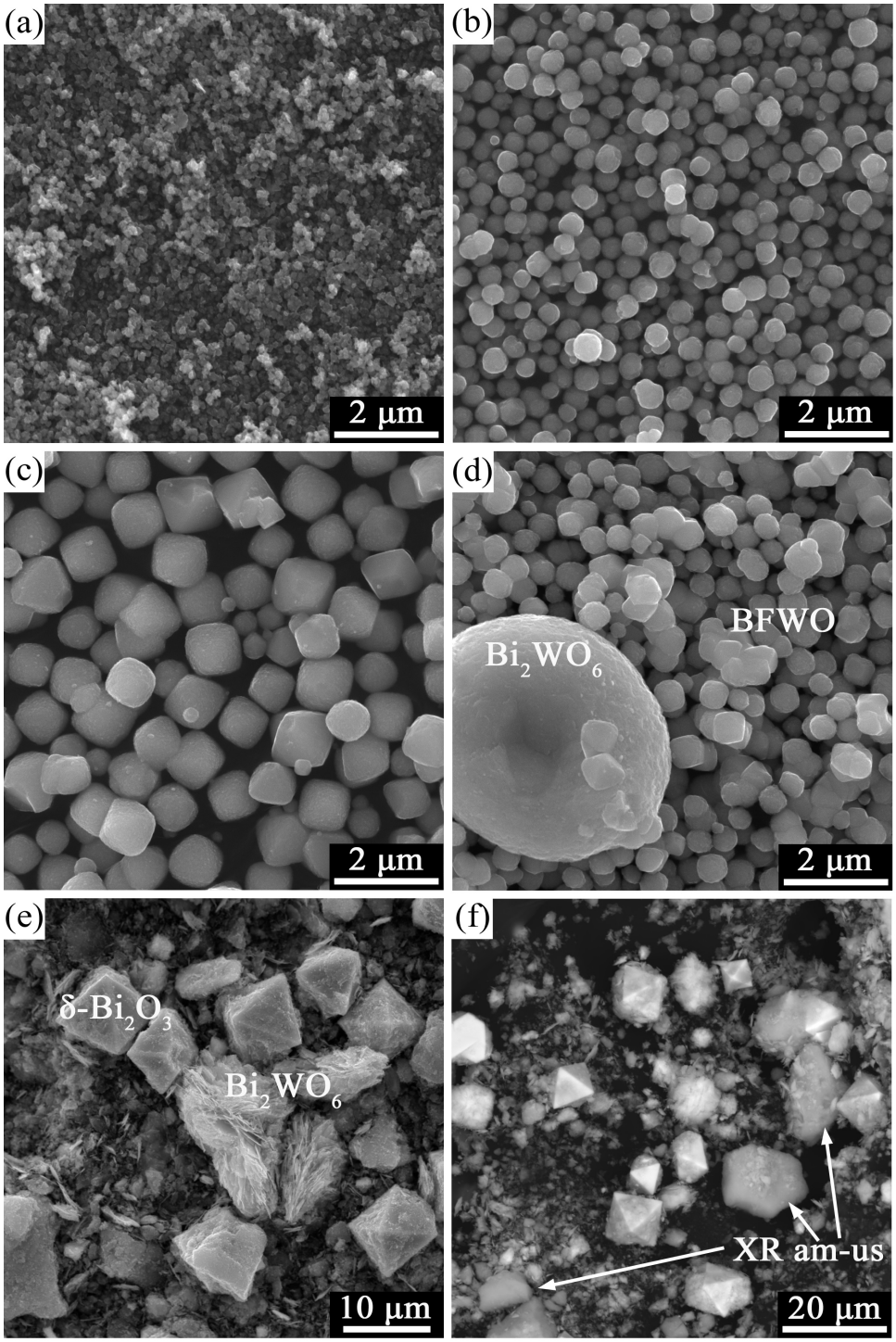

FIG. 4. SEM of the samples obtained at pH 1–(a), 3–(b), 5–(c), 8–(d), 10–(e) and 10–(BSE-detector)–(f)

4. Conclusion

A study of the effect that the hydrothermal fluid pH has on the BFWO phase formation under hydrothermal conditions showed that the phase state and composition of the individual phases in the HTS products in the water-salt system containing all three elements, i.e., Bi^{3+}, Fe^{3+}, and W^{6+}, significantly depend on the pH. It was found that the hydrothermal fluid pH significantly affects both the size of the BFWO phase crystallites and the size of the agglomerates consisting of them. It was shown for the studied initial composition that it is possible to obtain the BFWO phase with a composition specified for the synthesis only when the hydrothermal fluid pH equals 3–4.

Acknowledgments

XRD studies, SEM and EDXMA of samples were performed employing the equipment of the Engineering Center of the St. Petersburg State Institute of Technology.

References

[1] Almjasheva O.V., Smirnov A.V., Fedorov B.A., Tomkovich M.V., Gusarov V.V. Structural features of ZrO_2–Y_2O_3 and ZrO_2–Gd_2O_3 nanoparticles formed under hydrothermal conditions. *Russ. J. Gen. Chem.*, 2014, **84**(5), P. 804–809.

[2] Popkov V.I., Almjasheva O.V. Formation mechanism of $YFeO_3$ nanoparticles under the hydrothermal condition. *Nanosyst.:Phys. Chem. Math.*, 2014, **5**(5), P. 703–708.

[3] Almjasheva O.V., Gusarov V.V. Hydrothermal synthesis of nanosized and amorphous alumina in the ZrO_2-Al_2O_3-H_2O system. *Russ. J. Inorg. Chem.*, 2007, **52**(8), P. 1194–1200.

[4] Al'myasheva O.V., Korytkova E.N., Maslov A.V., Gusarov V.V. Preparation of Nanocrystalline Alumina under Hydrothermal Conditions. *Inorg. Mater.*, 2005, **41**(5), P. 460–467.

[5] Pozhidaeva O.V., Korytkova E.N., Romanov D.P., Gusarov V.V. Formation of ZrO_2 Nanocrystals in Hydrothermal Media of Various Chemical Compositions. *Russ. J. Gen. Chem.*, 2002, **72**(6), P. 849–853.

[6] Pozhidaeva O.V., Korytkova E.N., Drozdova I.A., Gusarov V.V. Phase state and particle size of ultradispersed zirconium dioxide as influenced by condition of hydrothermal synthesis. *Russ. J. Gen. Chem.*, 1999, **69**(8), P. 1219–1222.

[7] Kuznetsova V.A., Almjasheva O.V., Gusarov V.V. Influence of microwave and ultrasonic treatment on the formation of $CoFe_2O_4$ under hydrothermal conditions. *Glass Phys. Chem.*, 2009, **35**(2), P. 205–209.

[8] Proskurina O.V., Tomkovich M.V., Bachina A.K., Sokolov V.V., Danilovich D.P., Panchuk V.V., Semenov V.G., Gusarov V.V. Formation of Nanocrystalline $BiFeO_3$ under Hydrothermal Conditions. *Russ. J. Gen. Chem.*, 2017, **87**(11), P. 2507–2515.

[9] Almjasheva O.V., Krasilin A.A., Gusarov V.V. Formation mechanism of core-shell nanocrystals obtained via dehydration of coprecipitated hydroxides at hydrothermal conditions. *Nanosyst.: Phys. Chem. Math.*, 2018, **9**(4), P. 568–572.

[10] Krasilin A.A. Khrapova E.K. Effect of hydrothermal treatment conditions on formation of nickel hydrogermanate with platy morphology. *Russ. J. Appl. Chem.*, 2017, **90**(1), P. 22–27.

[11] Wang Y., Zhang S., Zhong Q., Zeng Y., Ou M., Cai W. Hydrothermal Synthesis of Novel Uniform Nanooctahedral $Bi_3(FeO_4)(WO_4)_2$ Solid Oxide and Visible-Light Photocatalytic Performance. *Ind. Eng. Chem. Res.*, 2016, **55**(49), P. 12539–12546.

[12] Bugrov A.N., Almjasheva O.V. Effect of hydrothermal synthesis conditions on the morphology of ZrO_2 nanoparticles. *Nanosyst.: Phys. Chem. Math.*, 2013, **4**(6), P. 810–815.

[13] Almjasheva O.V., Lomanova N.A., Popkov V.I., Proskurina O.V., Tugova E.A., Gusarov V.V. The minimum size of oxide nanocrystals: phenomenological thermodynamic vs crystal-chemical approaches. *Nanosyst.: Phys. Chem. Math.*, 2019, **10**(4), P. 428–437.

[14] Matveichuk Yu.V. FTIR-spectroscopic investigation of sodium tungstate and sodium molybdate solutions in wide range of H. *Izv. Vyssh. Uchebn. Zaved. Khim. Khim. Tekhnol.*, 2017, **60**(1), P. 56–63.

[15] Cornell R. M., Giovanoli R., Schneider W. Review of the hydrolysis of iron (III) and the crystallization of amorphous iron (III) hydroxide hydrate. *J. Chem. Tech. Biotechnol.*, 1989, **46**, P. 115–134.

[16] Yukhin Yu.M., Mikhailov Yu.I. Chemistry of bismuth compounds and materials. *SB RAS Publishing House*, Novosibirsk, 2001, 360 p.

[17] Lomakin M.S., Proskurina O.V., Danilovich D.P., Panchuk V.V., Semenov V.G., Gusarov V.V. Hydrothermal Synthesis, Phase Formation and Crystal Chemistry of the pyrochlore/Bi_2WO_6 and pyrochlore/α-Fe_2O_3 Composites in the Bi_2O_3-Fe_2O_3-WO_3 System. *J. Solid State Chem.*, 2020, **282**, 121064.